RPE | Radiation Physics & Engineering
An International Peer-Reviewed Journal
Published by K.N. Toosi University of Technology
http://rpe.kntu.ac.ir
Research Article

Radiation Physics and Engineering 2020; 1(3):17–27
https://doi.org/10.22034/RPE.2020.89328

# Flow regimes classification and prediction of volume fractions of the gas-oil-water three-phase flow using Adaptive Neuro-fuzzy Inference System

Gholam Hossein Roshani[a], Alimohammad Karami[b], Ehsan Nazemi[c], Cesar Marques Salgado[d,*]

[a] *Electrical Engineering Department, Kermanshah University of Technology, Kermanshah, Iran*
[b] *Mechanical Engineering Department, Razi University, Kermanshah, Iran*
[c] *Nuclear Science and Technology Research Institute, Tehran, Iran*
[d] *Instituto de Engenharia Nuclear, CNEN/IEN, P.O. Box 68550, 21945-970 Rio de Janeiro, Brazil*

## HIGHLIGHTS

- The MCNPX code provided data for training of ANFIS has been used.
- The methodology is based on dual energy broad-beam gamma-ray attenuation.
- ANFIS is used to classify the flow regimes and predict the volume fractions in multiphase systems.
- Water, gas and oil percentages in three flow regimes are obtained precisely with two detectors.

## ABSTRACT

The used metering technique in this study is based on the dual energy (Am-241 and Cs-137) gamma ray attenuation. Two transmitted NaI detectors in the best orientation were used and four features were extracted and applied to the model. This paper highlights the application of Adaptive Neuro-fuzzy Inference System (ANFIS) for identifying flow regimes and predicting volume fractions in gas-oil-water multiphase systems. In fact, the aim of the current study is to recognize the flow regimes based on dual energy broad-beam gamma-ray attenuation technique using ANFIS. In this study, ANFIS is used to classify the flow regimes (annular, stratified, and homogenous) and predict the value of volume fractions. To start modeling, sufficient data are gathered. Here, data are generated numerically using MCNPX code. In the next step, ANFIS must be trained. According to the modeling results, the proposed ANFIS can correctly recognize all the three different flow regimes, and other ANFIS networks can determine volume fractions with MRE of less than 2% according to the recognized regime, which shows that ANFIS can predict the results precisely.

## KEYWORDS

Three-phase flow
Pattern recognition
Volume fraction
Adaptive neuro-fuzzy inference system
Monte Carlo simulation

## HISTORY

Received: 16 October 2018
Revised: 6 December 2018
Accepted: 29 December 2018
Published: July 2020

## 1 Introduction

The world's high demand for oil and gas has been a motivation for petroleum companies to continually look for ways to develop oil and gas production techniques. Objectives have included making marginal fields more cost effective, establishing production facilities in difficult physical environments, reducing the development cost, and improving the energy efficiency of new fields (Thorn et al., 1997). The multiphase flowmeter plays an important role in these fields and all attempts which lead to improve this technique are important. In 1980, Abouelwafa and Kendall (Abouelwafa and Kendall, 1980) presented a novel method in order to measure the component ratios in multiphase systems using gamma ray attenuation. They found that gamma ray attenuation could be successfully used for three or more component systems to measure the component ratios. Since that time, many researchers have focused on this field and have improved that significantly. In 1993, Bishop and James analyzed the multiphase flows by dual-energy gamma densitometry and using neural networks for the first time (Bishop and James, 1993). They showed that neural network techniques, combined with dual-energy gamma densitometry, provide a powerful and accurate approach to the non-invasive analysis of multiphase flows and if there is insufficient information to perform a tomographic reconstruction of the phase configuration, a neural network can learn to distinguish between a finite number of previously characterized configurations with a high degree of discrimination.

*Corresponding author: otero@ien.gov.br

In 2009, Salgado *et al.* (Salgado et al., 2009) presented a methodology based on nuclear technique and ANN for volume fraction predictions in annular, stratified and homogeneous oil-water-gas regimes. Using principles of gamma-ray absorption and scattering together with an appropriate geometry, comprised of three detectors and a dual-energy gamma-ray source, it had been possible to obtain data, which could be Adequately correlated to the volume fractions of each phase by means of neural network. One year later, they presented a new methodology for flow regimes identification and volume fraction predictions in water-gas-oil multiphase systems based on gamma-ray pulse height distributions (PHDs) pattern recognition (Salgado et al., 2010).

In 2013, Multi-Layer Perceptron (MLP) was used in order to develop a gamma ray fluid densitometer in petroleum products monitoring application (Khorsandi et al., 2013). Trained Artificial Neural Network (ANN) model predicted the densities with Mean Relative Error (MRE) less than 0.5%. Roshani *et al.* (Roshani et al., 2014) presented the precise volume fraction prediction in oil-water-gas multiphase flows by means of gamma-ray attenuation and ANNs using a single detector. In this work, number of detectors and ANN input features were reduced to one and two, respectively. Cs-137 and Eu-152 were used as dual energy source and defined MRE was obtained less than 0.13%. In 2015, a method based on dual-modality densitometry was presented by Roshani *et al.*, which offers the advantage of the measurement of the oil-gas-water volume fractions independent of density changes (Roshani et al., 2015). Four features were extracted from the transmission and scattered detectors and were applied to the ANN as inputs. The input parameters comprised the Am-241 full energy peak, Cs-137 Compton edge, Cs-137 full energy peak and total scattered count, and the outputs were the oil and air volume fractions. MRE of the model was 0.7%.

The gas and oil percentages of a three phase flow have been obtained using Multi-Layer Perceptron. The used single network has four inputs and two outputs. Usage of more than one network or changing the sets of outputs (gas-oil, gas-water or oil-water) or using a new network like ANFIS can improve the precision of the presented system. It should be noted that in petroleum industry, the metering precision is of high importance (Roshani et al., 2017b,a). In 2016, a gamma-ray transmission technique was presented to measure the void fraction and to identify the flow regime of a two-phase flow using two detectors which were optimized in terms of detector orientation (Nazemi et al., 2016). The first detector was placed in direction of 0° and the second one was placed in direction of 13° with respect to the source based on the obtained optimum orientation determined by the simulations. The three idealistic flow regimes were determined correctly in gas-liquid two phase flows and the void fraction was predicted using two transmitted detectors with MRE less than 1.5%.

In the present study, based on the best obtained position in our previous work (Nazemi et al., 2016), a dual energy source and two transmitted detectors were used in three phase flows. Three different regimes (annular, stratified and homogenous) were considered and the volume fractions were obtained using ANFIS. To our knowledge, there is not a study on identifying flow regime in oil-water-gas three-phase flows by the use of Adaptive Neuro-fuzzy Inference System (ANFIS). In fact, the aim of the present work is to recognize the flow regimes based on dual energy broad-beam gamma-ray attenuation technique using ANFIS. In the present investigation, four ANFIS networks are applied to identify the flow regime and determine the volume fraction.

## 2 Methodology

### *2.1 Monte Carlo Simulation*

MCNPX is a Fortran90 Monte Carlo radiation transport computer code capable of tracking 34 particle types at nearly all energies. It is a production computer code for modeling the interaction of radiation with matter, and its quality is guaranteed (Pelowitz et al., 2005). This code has been used in several studies (Khorsandi et al., 2013; Roshani et al., 2014, 2015, 2017b). The detection geometry in the simulation is based on an experimental setup which was carried out in our previous study (Nazemi et al., 2016). In that work, the optimum positions for the two transmitted detectors for two phase flow were obtained using Monte Carlo simulation. Moreover, an experimental setup was constructed to identify flow regime and determine void fraction. The optimum positions of these NaI (Tl) detectors have been shown in Fig. 1. In this study, according to this setup, a metering system was simulated in three phase flow using dual energy gamma ray source. Am-241 was added to Cs-137 in order to construct dual energy gamma ray source. Cs-137 source (used in two phase flow meter) emits 662 keV photons which are sensitive to density and can distinguish the gas phase from liquid phase. Because of the close density of water and oil, the photons with photoelectric interactions (low energy) were needed in order to distinguish water from oil. Am-241 which emits 59.5 keV photons can identify oil from water phase (Roshani et al., 2014).

The three phase flow (gas-oil-water) in the pipe was simulated using MCNPX code in three different regimes (annular, homogenous and stratified). It should be noted that the number of counts correspond to the full energy peaks (FEP) of Am-241 and Cs-137 in both transmitted detectors, which are calculated per source particle using pulse height tally F8 in MCNPX code. A schematic view of simulated configuration in MCNPX code is shown in Fig. 2.

Applying Monte Carlo simulations, it was possible to generate an adequate data set for training and testing the intelligent models. The oil was assumed as a hydrocarbon (molecular formula $C_{12}H_{23}$) with density of 0.826 g.cm$^{-3}$. The gaseous phase was substituted by air, and the density of water was considered to be 1.0 g.cm$^{-3}$. The simulation results using MCNPX code have been tabulated in Table 1.

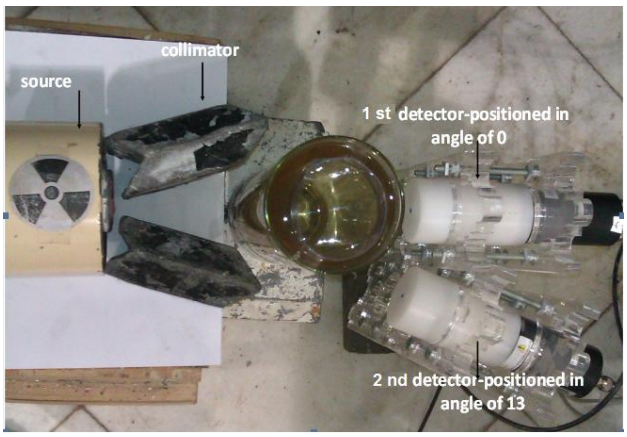


**Figure 1:** The optimized structure of two transmitted detectors.

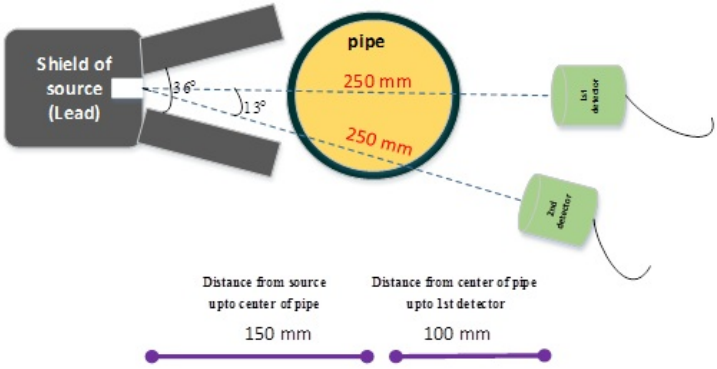


**Figure 2:** A schematic view of the simulated configuration.

### *2.2 Adaptive Neuro-fuzzy Inference Systems (ANFIS)*

ANFIS is a fuzzy inference system (Takagi and Sugeno, 1985; Jang et al., 1997; Jang and Sun, 1995; Gulley and Jang, 1995) implemented in the framework of neural networks (Amiri et al., 2012). This combination merges the advantages of fuzzy systems and neural networks. The main target of ANFIS is to find a model which can adjust the inputs with the outputs accurately.

Assume that the fuzzy inference system (FIS) has two inputs $(x, y)$ and one output $(f)$ (Karami et al., 2012; Yousefi et al., 2012; Karami et al., 2016; Aghakhani et al., 2012, 2014). For the first order Sugeno fuzzy model, a single fuzzy if-then rule assumes the form:

- Rule1: if $x$ is $A_1$ and $y$ is $B_1$, then $f_1 = p_1x+q_1y+r_1$
- Rule2: if $x$ is $A_2$ and $y$ is $B_2$, then $f_2 = p_2x+q_2y+r_2$

where $A_i$, $B_i$, and $f_i$ are fuzzy sets and system's output, respectively. Also $p_i$, $q_i$, and $r_i$ stand for designing parameters which are obtained during the training process for $i, j = 1, 2$. The reasoning mechanism for this Sugeno model is illustrated in Fig. 3.

The corresponding equivalent ANFIS architecture is also shown in Fig. 4. The layers shown in this figure are defined as follows:

- Layer 1: Every node in this layer is an adaptive node with a node function given by Eqs. (1) and (2):

$$Q_{1,i} = \mu_{A_i}(x), \quad i = 1, 2 \tag{1}$$

$$Q_{1,i} = \mu_{B_{i-2}}(x), \quad i = 3, 4 \tag{2}$$

  where $i$ is the membership grade of a fuzzy set $(A_1, A_2, B_1, B_2)$ and $Q_{1,i}$ is the output of the node $i$ in the layer 1.

- Layer 2: Every node in this layer is a fixed node label "Mult" ($\Pi$), the nodes multiply all incoming signals and the outputs are given by Eq. (3):

$$Q_{2,i} = w_i = \mu_{A_i}(x)\mu_{B_i}(y), \quad i = 1, 2 \tag{3}$$

  Each node in this layer represents the firing strength of a rule.

- Layer 3: Every node in this layer is a fixed node labeled "Norm" (N) which calculates the ratio of the $i^{th}$ rule's firing strength to the sum of all rule's firing strengths. The output of each node in this layer is called normalized firing strength and is given by Eq. (4):

$$Q_{3,i} = \overline{w}_i = \frac{w_i}{w_1 + w_2}, \quad i = 1, 2 \tag{4}$$

- Layer 4: In this layer, all nodes are adaptive nodes with a node function given by Eq. (5):

$$Q_{4,i} = \overline{w}_i f_i = \overline{w}_i(p_i x + q_i y + r_i), \quad i = 1, 2 \tag{5}$$

- Layer 5: This layer is a fixed node labeled "Sum" ($\Sigma$) computing the overall output as the summation of all incoming signals given by Eq. (6):

$$Q_{5,i} = \Sigma_i \overline{w}_i f_i = \frac{\Sigma_i w_i f_i}{\Sigma_i w_i}, \quad i = 1, 2 \tag{6}$$

In ANFIS structure, the parameters' sets are divided into two categories, one called adaptive parameters and the other called consequent parameters. If the modeling is carried out properly and using both sets of parameters, the difference between the predicted outputs and observed ones should give the lowest possible level of error. In this regard, ANFIS uses a hybrid algorithm to identify the parameters being a two-step process. In the first process, the adaptive parameter sets are assumed to be constant and the consequent parameter sets are calculated by least-squares method; this process is called forward pass. In the second process which is called backward pass, the consequent parameters are assumed to be constant and the adaptive parameters set is obtained by gradient descends method (Roshani et al., 2015). When the parameters sets of the model are obtained, the values of the model output can be calculated for each orderly pair of training data and can be compared with the values that have been anticipated by the model (Gulley and Jang, 1995). From the computational point of view, ANFIS can be regarded as a flexible mathematical structure that can be used for modeling and simulation in many engineering fields (Rezaei et al., 2012; Karami et al., 2013a,b, 2014, 2015, 2013c).

**Table 1:** Validated simulation results for different water and gas percentages using MCNPX code.

| Pattern | Flow Regime | Water (%) | Gas (%) | FEP Am-241 (D1) | FEP Cs-137 (D1) | FEP Am-241 (D2) | FEP Cs-137 (D2) |
|---|---|---|---|---|---|---|---|
| 1 | Annular | 80 | 10 | 9.13532E-05 | 2.46934E-05 | 7.10402E-05 | 1.93740E-05 |
| 2 | Annular | 70 | 10 | 9.56036E-05 | 2.52130E-05 | 7.15301E-05 | 1.93984E-05 |
| 3 | Annular | 60 | 10 | 9.78702E-05 | 2.54081E-05 | 7.26037E-05 | 1.93753E-05 |
| 4 | Annular | 50 | 10 | 1.00510E-04 | 2.55611E-05 | 7.43563E-05 | 1.94724E-05 |
| 5 | Annular | 40 | 10 | 1.02669E-04 | 2.59933E-05 | 7.68407E-05 | 1.95821E-05 |
| 6 | Annular | 30 | 10 | 1.04324E-04 | 2.62960E-05 | 7.99917E-05 | 1.99076E-05 |
| 7 | Annular | 20 | 10 | 1.05771E-04 | 2.63596E-05 | 8.24229E-05 | 2.02840E-05 |
| 8 | Annular | 10 | 10 | 1.07656E-04 | 2.64994E-05 | 8.45184E-05 | 2.05180E-05 |
| 9 | Annular | 70 | 20 | 1.11018E-04 | 2.73485E-05 | 7.19858E-05 | 1.94069E-05 |
| 10 | Annular | 60 | 20 | 1.13799E-04 | 2.76037E-05 | 7.29810E-05 | 1.93397E-05 |
| 11 | Annular | 50 | 20 | 1.16754E-04 | 2.78427E-05 | 7.47535E-05 | 1.94562E-05 |
| 12 | Annular | 40 | 20 | 1.19275E-04 | 2.81550E-05 | 7.72731E-05 | 1.95516E-05 |
| 13 | Annular | 30 | 20 | 1.21460E-04 | 2.83330E-05 | 8.05206E-05 | 1.98669E-05 |
| 14 | Annular | 20 | 20 | 1.23647E-04 | 2.85721E-05 | 8.28832E-05 | 2.02332E-05 |
| 15 | Annular | 10 | 20 | 1.25837E-04 | 2.87552E-05 | 8.49380E-05 | 2.04620E-05 |
| 16 | Annular | 60 | 30 | 1.27555E-04 | 2.93443E-05 | 7.32357E-05 | 1.92780E-05 |
| 17 | Annular | 50 | 30 | 1.31171E-04 | 2.96220E-05 | 7.48259E-05 | 1.94037E-05 |
| 18 | Annular | 40 | 30 | 1.34060E-04 | 2.98848E-05 | 7.73875E-05 | 1.94479E-05 |
| 19 | Annular | 30 | 30 | 1.36645E-04 | 3.01895E-05 | 8.08029E-05 | 1.98085E-05 |
| 20 | Annular | 20 | 30 | 1.38858E-04 | 3.02684E-05 | 8.31172E-05 | 2.01721E-05 |
| 21 | Annular | 10 | 30 | 1.40828E-04 | 3.04413E-05 | 8.48262E-05 | 2.03730E-05 |
| 22 | Annular | 50 | 40 | 1.44460E-04 | 3.12549E-05 | 0.000077743 | 1.97877E-05 |
| 23 | Annular | 40 | 40 | 1.47466E-04 | 3.15102E-05 | 7.97514E-05 | 1.98762E-05 |
| 24 | Annular | 30 | 40 | 1.49877E-04 | 0.00003184 | 8.28781E-05 | 2.02662E-05 |
| 25 | Annular | 20 | 40 | 1.52674E-04 | 3.20079E-05 | 8.51898E-05 | 2.06197E-05 |
| 26 | Annular | 10 | 40 | 1.54961E-04 | 3.21223E-05 | 8.70387E-05 | 2.09071E-05 |
| 27 | Annular | 40 | 50 | 1.60052E-04 | 3.31167E-05 | 8.76694E-05 | 2.15098E-05 |
| 28 | Annular | 30 | 50 | 1.62600E-04 | 3.33532E-05 | 9.09882E-05 | 2.19142E-05 |
| 29 | Annular | 20 | 50 | 1.65387E-04 | 3.35058E-05 | 9.37983E-05 | 2.21990E-05 |
| 30 | Annular | 10 | 50 | 1.68157E-04 | 3.37219E-05 | 0.000095431 | 2.25169E-05 |
| 31 | Annular | 30 | 60 | 1.75193E-04 | 3.48206E-05 | 0.000103657 | 2.37676E-05 |
| 32 | Annular | 20 | 60 | 1.78012E-04 | 3.50342E-05 | 0.000106997 | 2.41422E-05 |
| 33 | Annular | 10 | 60 | 1.80994E-04 | 3.52228E-05 | 0.000109025 | 2.45167E-05 |
| 34 | Annular | 20 | 70 | 1.90027E-04 | 3.62061E-05 | 0.000123019 | 2.62207E-05 |
| 35 | Annular | 10 | 70 | 1.93398E-04 | 0.000036393 | 0.000125935 | 2.64346E-05 |
| 36 | Annular | 10 | 80 | 2.04485E-04 | 3.75977E-05 | 0.00014169 | 2.85509E-05 |
| 37 | Homogenous | 80 | 10 | 7.57167E-05 | 2.20896E-05 | 8.23669E-05 | 2.14462E-05 |
| 38 | Homogenous | 70 | 10 | 7.81377E-05 | 2.23211E-05 | 8.42438E-05 | 2.16446E-05 |
| 39 | Homogenous | 60 | 10 | 8.01926E-05 | 2.25856E-05 | 8.61511E-05 | 2.18277E-05 |
| 40 | Homogenous | 50 | 10 | 8.26250E-05 | 2.29908E-05 | 8.81708E-05 | 2.19810E-05 |
| 41 | Homogenous | 40 | 10 | 8.50941E-05 | 2.32405E-05 | 8.99630E-05 | 2.21363E-05 |
| 42 | Homogenous | 30 | 10 | 8.78102E-05 | 2.35235E-05 | 9.21853E-05 | 2.23111E-05 |
| 43 | Homogenous | 20 | 10 | 9.02821E-05 | 2.37871E-05 | 9.40247E-05 | 2.24887E-05 |
| 44 | Homogenous | 10 | 10 | 9.32589E-05 | 2.40479E-05 | 9.62164E-05 | 2.26801E-05 |
| 45 | Homogenous | 70 | 10 | 8.54714E-05 | 2.37455E-05 | 9.04097E-05 | 2.24720E-05 |
| 46 | Homogenous | 60 | 20 | 8.80460E-05 | 2.39979E-05 | 9.24045E-05 | 2.26662E-05 |
| 47 | Homogenous | 50 | 20 | 9.06150E-05 | 2.43170E-05 | 9.43493E-05 | 2.28549E-05 |
| 48 | Homogenous | 40 | 20 | 9.32395E-05 | 2.45833E-05 | 9.62968E-05 | 2.30768E-05 |
| 49 | Homogenous | 30 | 20 | 9.60416E-05 | 2.49051E-05 | 9.82666E-05 | 2.32183E-05 |
| 50 | Homogenous | 20 | 20 | 9.89463E-05 | 2.52297E-05 | 1.00522E-04 | 2.33959E-05 |
| 51 | Homogenous | 10 | 20 | 1.02087E-04 | 2.55210E-05 | 1.03088E-04 | 2.35540E-05 |
| 52 | Homogenous | 60 | 30 | 9.64688E-05 | 2.54766E-05 | 9.85524E-05 | 2.35291E-05 |
| 53 | Homogenous | 50 | 30 | 9.91599E-05 | 2.57346E-05 | 1.00786E-04 | 2.37038E-05 |
| 54 | Homogenous | 40 | 30 | 1.02203E-04 | 2.60565E-05 | 1.03244E-04 | 2.39202E-05 |
| 55 | Homogenous | 30 | 30 | 1.05591E-04 | 2.63589E-05 | 1.05397E-04 | 2.41006E-05 |

**Table 1:** Continued.

| Pattern | Flow Regime | Water (%) | Gas (%) | FEP Am-241 (D1) | FEP Cs-137 (D1) | FEP Am-241 (D2) | FEP Cs-137 (D2) |
|---|---|---|---|---|---|---|---|
| 56 | Homogenous | 20 | 30 | 1.08777E-04 | 2.66113E-05 | 1.07413E-04 | 2.43195E-05 |
| 57 | Homogenous | 10 | 30 | 1.12485E-04 | 2.68341E-05 | 1.09854E-04 | 2.44873E-05 |
| 58 | Homogenous | 50 | 40 | 1.09332E-04 | 2.71240E-05 | 1.07870E-04 | 2.46246E-05 |
| 59 | Homogenous | 40 | 40 | 1.12820E-04 | 2.74902E-05 | 1.09888E-04 | 2.48199E-05 |
| 60 | Homogenous | 30 | 40 | 1.16104E-04 | 2.78534E-05 | 1.11942E-04 | 2.50305E-05 |
| 61 | Homogenous | 20 | 40 | 1.20062E-04 | 2.81921E-05 | 1.14523E-04 | 2.52380E-05 |
| 62 | Homogenous | 10 | 40 | 1.23654E-04 | 2.84637E-05 | 1.17355E-04 | 2.54578E-05 |
| 63 | Homogenous | 40 | 50 | 1.24283E-04 | 2.90344E-05 | 1.17365E-04 | 2.58209E-05 |
| 64 | Homogenous | 30 | 50 | 1.27939E-04 | 2.93900E-05 | 1.19529E-04 | 2.60395E-05 |
| 65 | Homogenous | 20 | 50 | 1.32347E-04 | 2.96920E-05 | 1.22074E-04 | 2.62419E-05 |
| 66 | Homogenous | 10 | 50 | 1.36744E-04 | 3.01096E-05 | 1.24631E-04 | 2.64732E-05 |
| 67 | Homogenous | 30 | 60 | 1.41788E-04 | 3.11376E-05 | 1.27727E-04 | 2.70225E-05 |
| 68 | Homogenous | 20 | 60 | 1.45701E-04 | 3.15263E-05 | 1.30169E-04 | 2.72377E-05 |
| 69 | Homogenous | 10 | 60 | 1.50557E-04 | 3.16840E-05 | 1.33080E-04 | 2.74014E-05 |
| 70 | Homogenous | 20 | 70 | 1.60512E-04 | 3.30777E-05 | 1.39038E-04 | 2.82220E-05 |
| 71 | Homogenous | 10 | 70 | 1.65612E-04 | 3.34981E-05 | 1.41669E-04 | 2.84729E-05 |
| 72 | Homogenous | 10 | 80 | 1.81989E-04 | 3.52999E-05 | 1.50843E-04 | 2.96595E-05 |
| 73 | Stratified | 80 | 10 | 7.41308E-05 | 2.16792E-05 | 6.99617E-05 | 1.92345E-05 |
| 74 | Stratified | 70 | 10 | 7.60771E-05 | 2.19439E-05 | 7.12539E-05 | 1.98778E-05 |
| 75 | Stratified | 60 | 10 | 7.81557E-05 | 2.21699E-05 | 7.25300E-05 | 1.99749E-05 |
| 76 | Stratified | 50 | 10 | 7.98492E-05 | 2.23058E-05 | 7.43230E-05 | 1.99585E-05 |
| 77 | Stratified | 40 | 10 | 8.18481E-05 | 2.25525E-05 | 7.60167E-05 | 2.02281E-05 |
| 78 | Stratified | 30 | 10 | 8.38318E-05 | 2.27763E-05 | 7.85395E-05 | 2.04290E-05 |
| 79 | Stratified | 20 | 10 | 8.62198E-05 | 2.30331E-05 | 8.07343E-05 | 2.06223E-05 |
| 80 | Stratified | 10 | 20 | 8.95157E-05 | 2.34426E-05 | 8.32011E-05 | 2.08079E-05 |
| 81 | Stratified | 70 | 20 | 8.38869E-05 | 2.32480E-05 | 7.37723E-05 | 2.02170E-05 |
| 82 | Stratified | 60 | 20 | 8.61410E-05 | 2.34833E-05 | 7.50529E-05 | 2.02560E-05 |
| 83 | Stratified | 50 | 20 | 8.82823E-05 | 2.36791E-05 | 7.66678E-05 | 2.04264E-05 |
| 84 | Stratified | 40 | 20 | 9.01489E-05 | 2.39690E-05 | 7.83437E-05 | 2.05866E-05 |
| 85 | Stratified | 30 | 20 | 9.23945E-05 | 2.40784E-05 | 8.08055E-05 | 2.08079E-05 |
| 86 | Stratified | 20 | 20 | 9.51284E-05 | 2.44980E-05 | 8.31807E-05 | 2.11334E-05 |
| 87 | Stratified | 10 | 20 | 9.82310E-05 | 2.47701E-05 | 8.54289E-05 | 2.12326E-05 |
| 88 | Stratified | 60 | 30 | 9.37983E-05 | 2.48260E-05 | 8.07699E-05 | 2.07265E-05 |
| 89 | Stratified | 50 | 30 | 9.63109E-05 | 2.49939E-05 | 8.21508E-05 | 2.09045E-05 |
| 90 | Stratified | 40 | 30 | 9.83887E-05 | 2.51973E-05 | 8.38954E-05 | 2.10419E-05 |
| 91 | Stratified | 30 | 30 | 1.00596E-04 | 2.54796E-05 | 8.61791E-05 | 2.12021E-05 |
| 92 | Stratified | 20 | 30 | 1.03378E-04 | 2.57187E-05 | 8.89079E-05 | 2.15174E-05 |
| 93 | Stratified | 10 | 30 | 1.06809E-04 | 2.61119E-05 | 9.16609E-05 | 2.17701E-05 |
| 94 | Stratified | 50 | 40 | 1.04396E-04 | 2.63138E-05 | 8.95208E-05 | 2.21405E-05 |
| 95 | Stratified | 40 | 40 | 1.06803E-04 | 2.65447E-05 | 9.12143E-05 | 2.22862E-05 |
| 96 | Stratified | 30 | 40 | 1.09447E-04 | 2.67445E-05 | 9.34615E-05 | 2.24471E-05 |
| 97 | Stratified | 20 | 40 | 1.12208E-04 | 2.71052E-05 | 9.61692E-05 | 2.26579E-05 |
| 98 | Stratified | 10 | 40 | 1.15939E-04 | 2.73798E-05 | 9.99229E-05 | 2.30491E-05 |
| 99 | Stratified | 40 | 50 | 1.15343E-04 | 2.78681E-05 | 9.92765E-05 | 2.34958E-05 |
| 100 | Stratified | 30 | 50 | 1.18786E-04 | 2.81261E-05 | 1.01649E-04 | 2.36622E-05 |
| 101 | Stratified | 20 | 50 | 1.21676E-04 | 2.84008E-05 | 1.045250E-04 | 2.39008E-05 |
| 102 | Stratified | 10 | 50 | 1.25203E-04 | 2.87392E-05 | 1.079820E-04 | 2.41671E-05 |
| 103 | Stratified | 30 | 60 | 1.28668E-04 | 2.93274E-05 | 1.107420E-04 | 2.48901E-05 |
| 104 | Stratified | 20 | 60 | 1.32257E-04 | 2.96844E-05 | 1.135040E-04 | 2.51251E-05 |
| 105 | Stratified | 10 | 60 | 1.36069E-04 | 2.99469E-05 | 1.167420E-04 | 2.54211E-05 |
| 106 | Stratified | 20 | 70 | 1.44403E-04 | 3.13046E-05 | 1.249780E-04 | 2.65824E-05 |
| 107 | Stratified | 10 | 70 | 1.48608E-04 | 3.15391E-05 | 1.285820E-04 | 2.69037E-05 |
| 108 | Stratified | 10 | 80 | 1.61808E-04 | 3.31489E-05 | 1.404280E-04 | 2.83847E-05 |

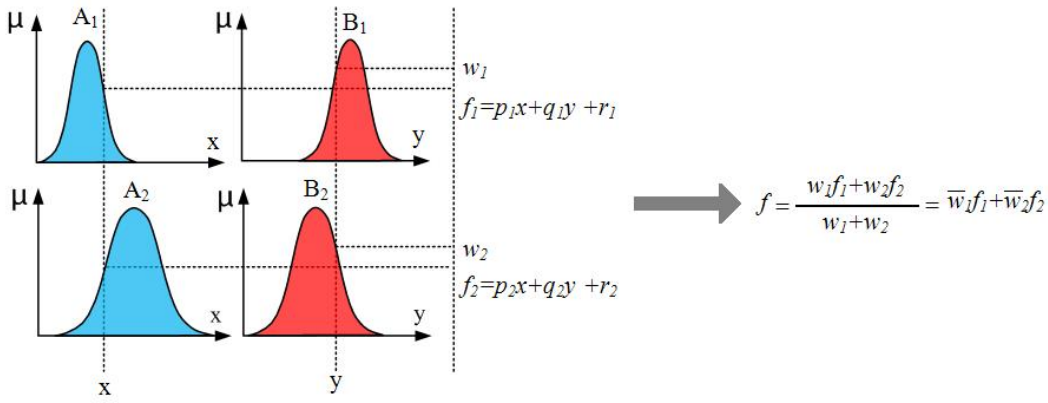


**Figure 3:** The inference method of Sugeno model.

In this study, at first an ANFIS network was used in order to recognize the flow regime. The specifications of this network are given in the pattern recognition section. Then, according to determined regime, the volume fractions of each phase were measured using three independent networks. The characteristics of these networks are given in the volume fraction determination section.

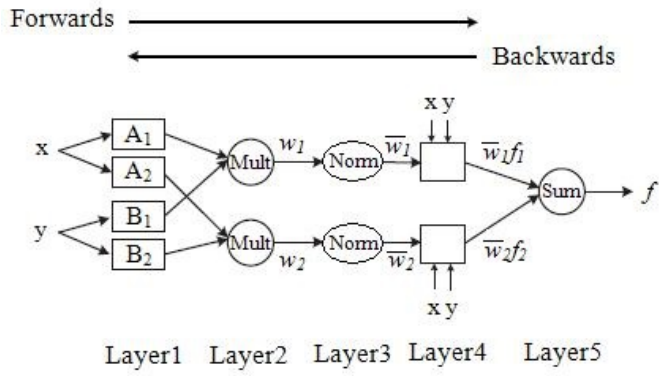


**Figure 4:** ANFIS architecture based on Takagi-Sugeno.

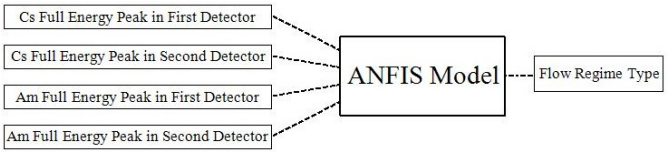


**Figure 5:** A simplified overview of the proposed ANFIS model in order to determine the flow regime.

### 2.2.1 Pattern recognition

In the present study, the ANFIS networks were developed with four specific peaks which were extracted as inputs. The proposed ANFIS models were developed and trained with MATLAB 8.1.0.604 software. A schematic view of the applied ANFIS model in order to determine the flow regime has been shown in Fig. 5, in which the ANFIS model was developed with four specific peaks related to Am-241 and Cs-137 in both transmitted detectors as inputs and the flow regime as desired output.

For developing the proposed ANFIS model 108 data were used. The whole data are divided into three sets: training, testing and evaluating. About 60% of the data (65 data) were selected for training, 30% (32 data) were selected for testing and the remained 10% of the whole data (11 data) were selected for evaluating the proposed ANFIS model. Training and testing sets were chosen randomly. To obtain the optimal ANFIS model, several structures have been constructed and tested. All of the flow regimes were distinguished correctly in both training and testing set.

### 2.2.2 Volume fraction determination

For determining the volume fractions, three independent models according to distinguished flow regime were presented. The inputs of these models were same as the pattern recognition model inputs. The schematic view of the proposed ANFIS models have been shown in Fig. 6, where the ANFIS models are developed with four specific peaks related to Am-241 and Cs-137 in both transmitted detectors as inputs and the water and gas volume fractions as desired outputs.

In order to develop the proposed ANFIS models for all flow regimes, 36 data were used. The procedure for volume fraction predicting was similar to pattern recognition procedure. The whole data are divided into three sets: training, testing and evaluating. About 60% of the whole data (22 data) were selected for training, 30% for testing (10 data) and the rest 10% (4 data) were selected for evaluating the proposed ANFIS models. Training and testing sets were chosen randomly. The best architectures of proposed ANFIS models for predicting the volume fractions are presented in Table 2.

## 3 Results and discussion

All of the regimes were predicted correctly for both training and testing set. Figure 7 shows the comparison between the predicted values using annular regime ANFIS model and validated simulated values using MCNPX code

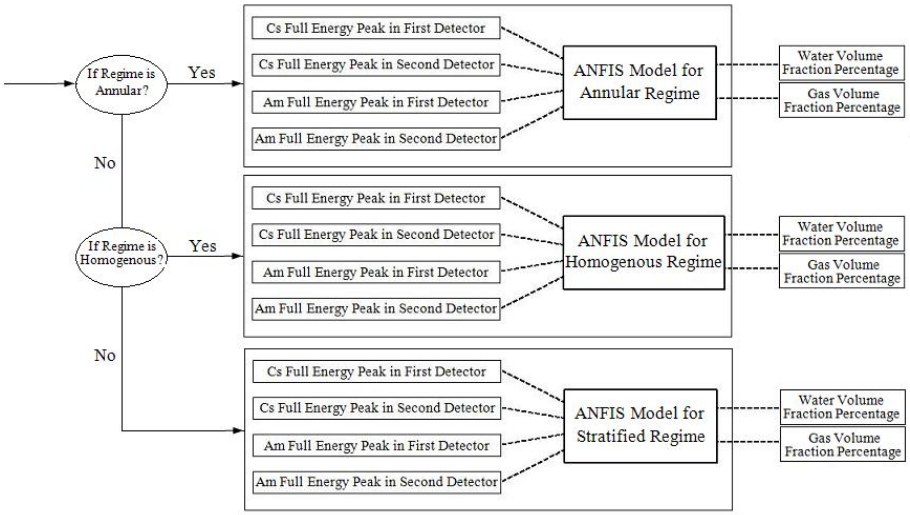


**Figure 6:** A simplified overview of the proposed ANFIS models in order to predict volume fraction percentages.

**Table 2:** Optimal architectures and specifications of proposed ANFIS models for predicting the volume fractions.

| The architecture of ANFIS | Annular Regime | Homogenous Regime | Stratified Regime |
|---|---|---|---|
| Type of fuzzy inference system (FIS) | Sugeno | Sugeno | Sugeno |
| Inputs/Output | 4/2 | 4/2 | 4/2 |
| Input membership function types | Gaussian | Gaussian | Gaussian |
| Output membership function types | Linear | Linear | Linear |
| Number of input membership functions | 7/7/7/7 | 6/6/6/6 | 9/9/9/9 |
| Number of output membership functions | 2401 | 1296 | 6561 |
| Rules Weight | 1 | 1 | 1 |
| Number of fuzzy rules | 2401 | 1292 | 6561 |
| Number of linear parameters | 56 | 50 | 56 |
| Number of nonlinear parameters | 29 | 21 | 29 |
| Number of epochs | 360 | 380 | 330 |

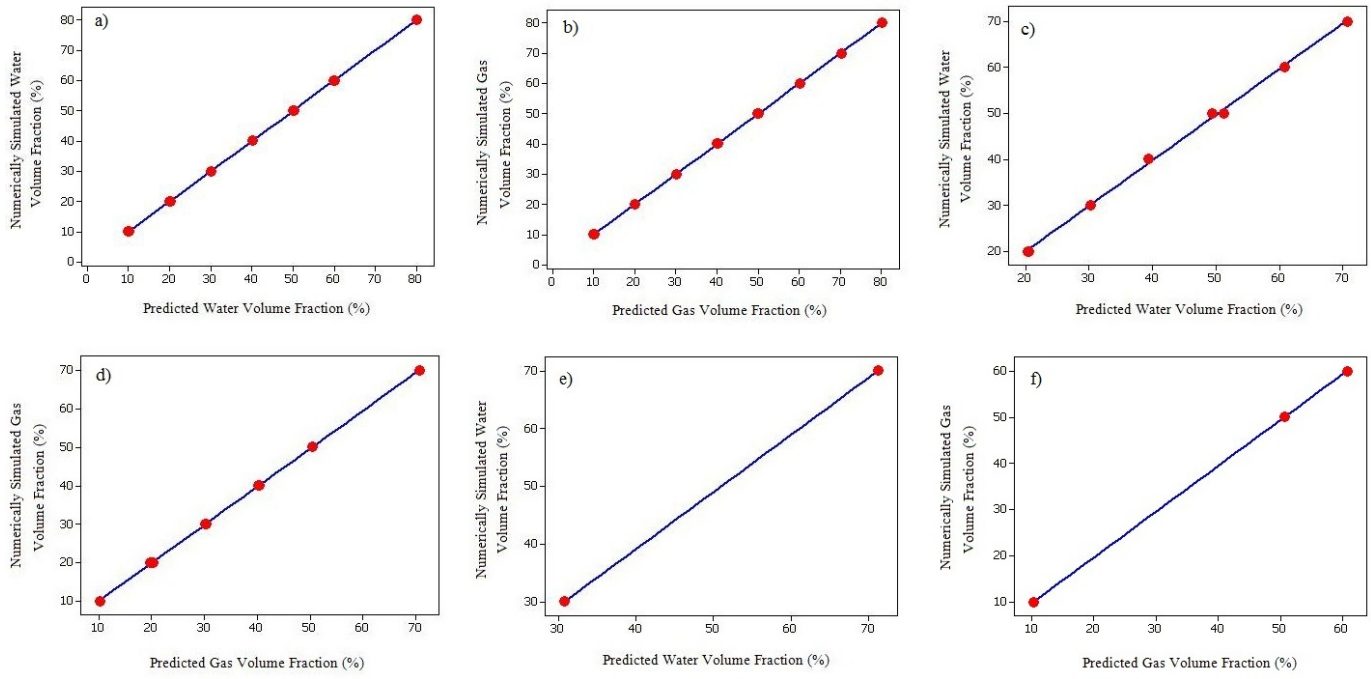


**Figure 7:** Comparisons between the numerically simulated and the ANFIS model results in annular regime for: a) training set water output, b) training set gas output, c) testing set water output, d) testing set gas output, e) evaluating set water output, f) evaluating set gas output.

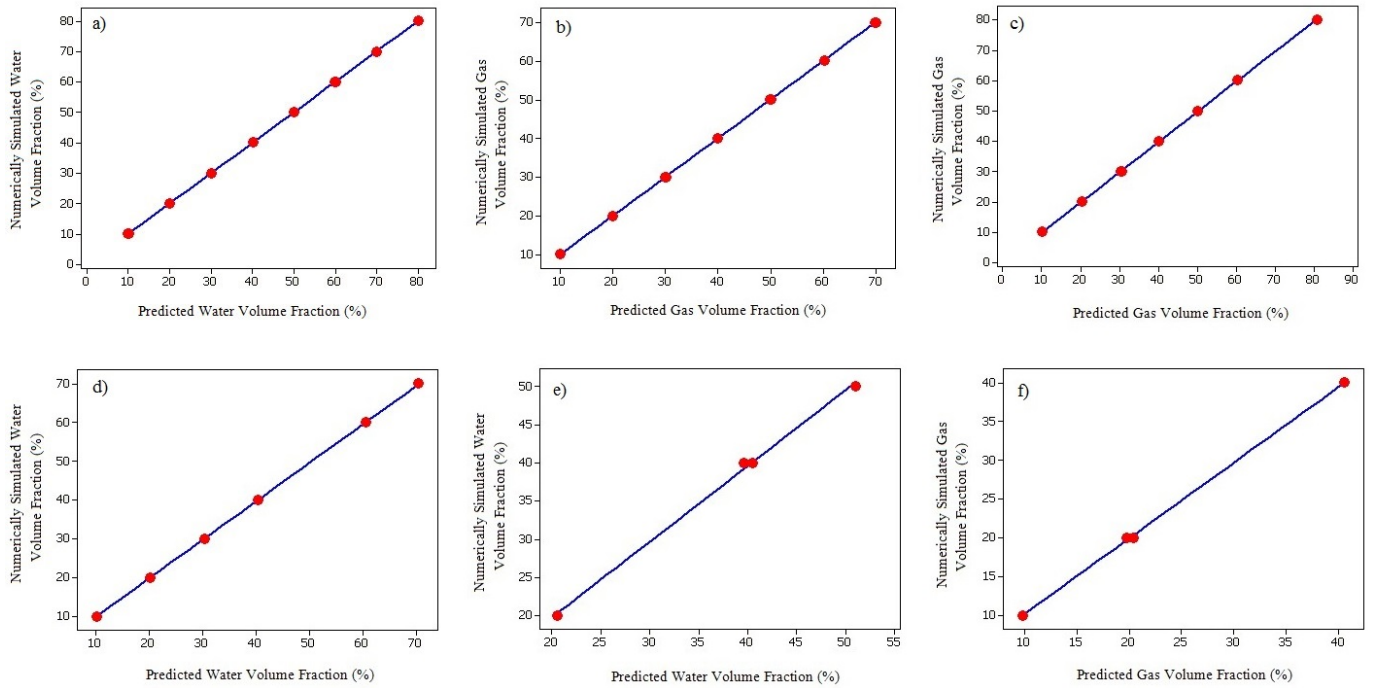


**Figure 8:** Comparisons between the numerically simulated and the ANFIS model results in homogenous regime for: a) training set water output, b) training set gas output, c) testing set water output, d) testing set gas output, e) evaluating set water output, f) testing set gas output.

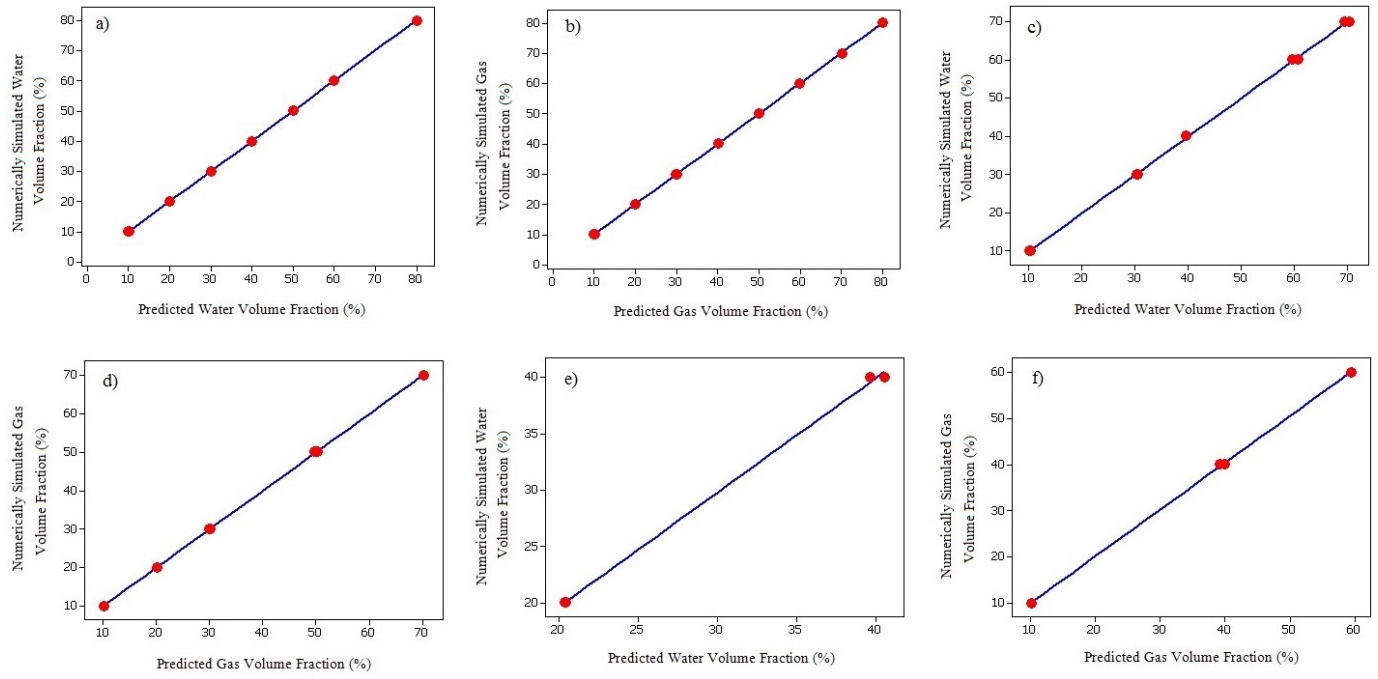


**Figure 9:** Comparisons between the numerically simulated and the ANFIS model results in stratified regime for: a) training set water output, b) training set gas output, c) testing set water output, d) testing set gas output, e) evaluating set water output, f) testing set gas output.

**Table 3:** The accuracy of the proposed ANFIS models in comparison with the numerically simulated results.

| Pattern | | Annular Regime | | | | Homogenous Regime | | | | Stratified Regime | | | |
|---|---|---|---|---|---|---|---|---|---|---|---|---|---|
| | | Water Volume Fraction | | Gas Volume Fraction | | Water Volume Fraction | | Gas Volume Fraction | | Water Volume Fraction | | Gas Volume Fraction | |
| | | MRE (%) | MAE | MRE (%) | MAE | MRE (%) | MAE | MRE (%) | MAE | MRE (%) | MAE | MRE (%) | MAE |
| Training | Min | 0.00 | 0.00 | 0.00 | 0.00 | 0.00 | 0.00 | 0.00 | 0.00 | 0.00 | 0.00 | 0.00 | 0.00 |
| | Max | 1.00 | 0.15 | 0.50 | 0.25 | 0.16 | 0.10 | 0.50 | 0.20 | 0.50 | 0.15 | 0.21 | 0.15 |
| | Mean | 0.23 | 0.05 | 0.29 | 0.09 | 0.15 | 0.05 | 0.17 | 0.05 | 0.21 | 0.05 | 0.20 | 0.06 |
| Testing | Min | 1.14 | 1.20 | 0.50 | 0.10 | 0.71 | 0.15 | 0.40 | 0.10 | 0.50 | 0.05 | 0.16 | 0.05 |
| | Max | 2.40 | 0.30 | 2.00 | 0.80 | 2.50 | 0.70 | 1.66 | 0.9 | 2.00 | 0.30 | 1.00 | 0.35 |
| | Mean | 1.52 | 0.60 | 1.01 | 0.31 | 1.43 | 0.38 | 1.12 | 0.36 | 1.08 | 0.16 | 0.53 | 0.16 |
| Evaluating | Min | 1.85 | 0.70 | 1.40 | 0.20 | 1.00 | 0.40 | 1.00 | 0.20 | 0.87 | 0.10 | 0.25 | 0.10 |
| | Max | 2.66 | 1.30 | 2.50 | 0.90 | 3.00 | 1.00 | 2.00 | 0.60 | 2.00 | 0.25 | 2.00 | 0.80 |
| | Mean | 2.29 | 0.87 | 1.85 | 0.51 | 1.80 | 0.62 | 1.62 | 0.35 | 1.53 | 0.15 | 1.14 | 0.38 |

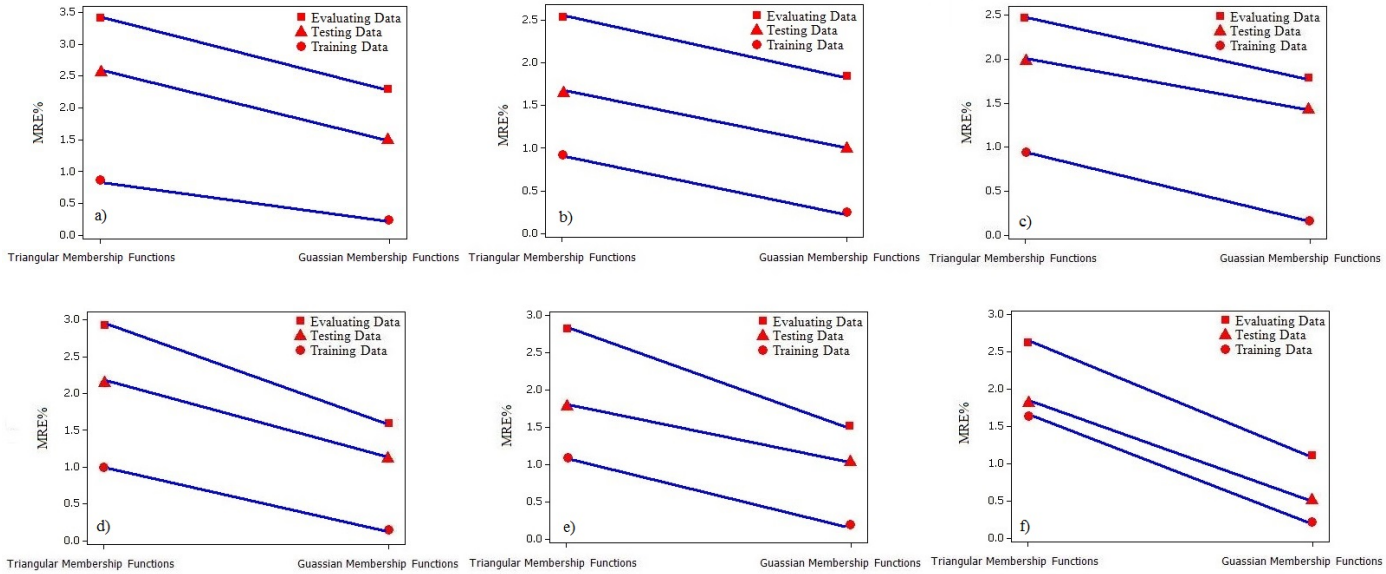


**Figure 10:** The MRE of the ANFIS model against the type of membership functions for: a) water output in annular regime, b) gas output in annular regime, c) water output in homogenous regime, d) gas output in homogenous regime, e) water output in stratified regime, f) gas output in stratified regime.

**Table 4:** Optimal architectures and specifications of the compared ANFIS models for predicting the volume fractions.

| The architecture of ANFIS | Annular Regime | Homogenous Regime | Stratified Regime |
|---|---|---|---|
| Type of fuzzy inference system (FIS) | Sugeno | Sugeno | Sugeno |
| Inputs/Output | 4/2 | 4/2 | 4/2 |
| Input membership function types | Triangular | Triangular | Triangular |
| Output membership function types | Linear | Linear | Linear |
| Number of input membership functions | 8/8/8/8 | 7/7/7/7 | 8/8/8/8 |
| Number of output membership functions | 4096 | 2401 | 4096 |
| Rules Weight | 1 | 1 | 1 |
| Number of fuzzy rules | 4096 | 2401 | 4096 |
| Number of linear parameters | 44 | 43 | 50 |
| Number of nonlinear parameters | 23 | 19 | 21 |
| Number of epochs | 395 | 415 | 375 |

for both training and testing data in annular regime. From this figure, it is clear that the predicted values using the proposed ANFIS model are in good agreement with simulated data with least error. Figures 8 and 9 show these comparisons in homogenous and stratified regimes, respectively.

The mean relative error percentage (MRE%) and the mean absolute error (MAE) of the proposed ANFIS models are calculated by Eqs. (7) and (8), where $N$ is the number of data and $O_{Num,i}$ and $O_{Pred,i}$ stand for numerical simulation (MCNPX) and predicted values, respectively.

$$MRE(\%) = \frac{1}{N}\sum_{i=1}^{N} \mid \frac{O_{Num,i} - O_{Pred,i}}{O_{Num,i}} \mid \times 100 \qquad (7)$$

$$MAE = \frac{1}{N}\sum_{i=1}^{N} \mid O_{Num,i} - O_{Pred,i} \mid \qquad (8)$$

The error information of the proposed ANFIS models in predicting the volume fraction percentages of water and gas are presented in Table 3. According to this table, in the annular regime and training set, MRE% and MAE for predicting the water output are 0.23% and 0.05, respectively. These values are 0.26% and 0.09 for the gas output. Also, for the testing set, these errors for water output are 1.52% and 0.6, respectively, and 1.01% and 0.31 for the gas output. In the homogenous regime and training set, MRE% and MAE for predicting the water output are 0.15% and 0.05, respectively, and 0.17% and 0.05 for the gas output. Additionally, for the testing set these errors for water output are 1.43% and 0.38, respectively, and 1.12% and 0.36 for the gas output. In the stratified regime and training set, MRE% and MAE for predicting the water output are 0.21% and 0.05, respectively, and 0.23% and 0.06 for the gas output. Moreover, for the testing set these errors for water output are 1.08% and 0.16, respectively, and 0.53% and 0.16 for the gas output.

It is worth mentioning that the aforementioned ANFIS models has been trained and tested using triangular membership functions in addition to Gaussian membership functions. The results are shown in Fig. 10. As can be observed from these figures, for testing data, using Gaussian membership functions, leads to lower values of error. For example, using Gaussian membership functions, leads to 41% decrease in MRE% with respect to similar one by triangular memberships, for predicting the water volume fraction in annular regime. This decrement in MRE for water volume fraction is 28% and 42% in homogenous and stratified regimes. Additionally, for gas volume fraction, 39%, 49%, and 17% decrement in MRE is occurred for annular, homogenous, and stratified regimes, respectively. Generally, it can be concluded that using Gaussian membership functions helps ANFIS models to predict the results more accurate.

Specifications of the compared ANFIS models in which triangular memberships are applied have been presented in Table 4.

## 4 Conclusions

In this study, water, gas, and oil percentages in annular, homogenous and stratified regimes were obtained precisely using two transmitted detectors which led to less metering time. Four features (Am-241 and Cs-137 full energy peaks in both detectors) from output signals of both detectors were extracted. Four accurate and precise ANFIS models were developed. The first one was used in order to determine the type of three-phase flow regime. All of the regimes were recognized correctly. Then, according to distinguished regime, three independent ANFIS models were used in order to predict the volume fraction percentages of gas, oil, and water. The networks were developed based on the validated numerical simulated data from MCNPX code. The comparison between numerically simulated values and predicted ones showed that there is an acceptable agreement between them with the least possible error. The volume fractions were measured with MRE% of less than 2% for the all data. Based on the results, it can be concluded that the proposed ANFIS models are reliable flexible mathematical structures for prediction of the results due to their high accuracy. They can therefore be used to predict the results precisely.

## References

Abouelwafa, M. and Kendall, E. (1980). The measurement of component ratios in multiphase systems using alpha-ray attenuation. *Journal of Physics E: Scientific Instruments*, 13(3):341.

Aghakhani, M., Ghaderi, M., Karami, A., et al. (2014). Combined effect of $TiO_2$ nanoparticles and input welding parameters on the weld bead penetration in submerged arc welding process using fuzzy logic. *The International Journal of Advanced Manufacturing Technology*, 70(1-4):63–72.

Aghakhani, M., Jalilian, M. M., and Karami, A. (2012). Prediction of weld bead dilution in GMAW process using fuzzy logic. In *Applied Mechanics and Materials*, volume 110, pages 3171–3175. Trans Tech Publ.

Amiri, A., Karami, A., Yousefi, T., and Zanjani, M. (2012). Artificial neural network to predict the natural convection from vertical and inclined arrays of horizontal cylinders. *Polish Journal of Chemical Technology*, 14(4):46–52.

Bishop, C. M. and James, G. D. (1993). Analysis of multiphase flows using dual-energy gamma densitometry and neural networks. *Nuclear Instruments and Methods in Physics Research Section A: Accelerators, Spectrometers, Detectors and Associated Equipment*, 327(2-3):580–593.

Gulley, N. and Jang, J.-S. R. (1995). Fuzzy logic toolbox user's guide. *The MathWorks, Inc*, 24.

Jang, J., Sun, C., and Mizutani, E. (1997). Neuro-fuzzy and soft computing,(1997). *PTR Prentice Hall*.

Jang, J.-S. and Sun, C.-T. (1995). Neuro-fuzzy modeling and control. *Proceedings of the IEEE*, 83(3):378–406.

Karami, A., Akbari, E., Rezaei, E., et al. (2013a). Neuro-fuzzy modeling of the free convection from vertical arrays of isothermal cylinders. *Journal of Thermophysics and Heat Transfer*, 27(3):588–592.

Karami, A., Rezaei, E., Rahimi, M., et al. (2013b). Modeling of heat transfer in an air cooler equipped with classic twisted tape inserts using adaptive neuro-fuzzy inference system. *Chemical Engineering Communications*, 200(4):532–542.

Karami, A., Rezaei, E., Shahhosseni, M., et al. (2012). Fuzzy logic to predict the heat transfer in an air cooler equipped with different tube inserts. *International Journal of Thermal Sciences*, 53:141–147.

Karami, A., Yousefi, T., Ebrahimi, S., et al. (2013c). Adaptive neuro-fuzzy inference system (ANFIS) to predict the forced convection heat transfer from a v-shaped plate. *Heat and Mass Transfer*, 49(6):789–798.

Karami, A., Yousefi, T., Harsini, I., et al. (2015). Neuro-fuzzy modeling of the free convection heat transfer from a wavy surface. *Heat Transfer Engineering*, 36(9):847–855.

Karami, A., Yousefi, T., Mohebbi, S., et al. (2014). Prediction of free convection from vertical and inclined rows of horizontal isothermal cylinders using ANFIS. *Arabian Journal for Science and Engineering*, 39(5):4201–4209.

Karami, A., Yousefi, T., Rezaei, E., et al. (2016). Modeling of the free convection heat transfer from an isothermal horizontal cylinder in a vertical channel via the fuzzy logic. *The International Journal of Multiphysics*, 6(1).

Khorsandi, M., Feghhi, S., Salehizadeh, A., et al. (2013). Developing a gamma ray fluid densitometer in petroleum products monitoring applications using Artificial Neural Network. *Radiation Measurements*, 59:183–187.

Nazemi, E., Roshani, G., Feghhi, S., et al. (2016). Optimization of a method for identifying the flow regime and measuring void fraction in a broad beam gamma-ray attenuation technique. *International Journal of Hydrogen Energy*, 41(18):7438–7444.

Pelowitz, D. B. et al. (2005). MCNPXTM user's manual. *Los Alamos National Laboratory, Los Alamos*.

Rezaei, E., Karami, A., Yousefi, T., et al. (2012). Modeling the free convection heat transfer in a partitioned cavity using ANFIS. *International Communications in Heat and Mass Transfer*, 39(3):470–475.

Roshani, G., Feghhi, S., Mahmoudi-Aznaveh, A., et al. (2014). Precise volume fraction prediction in oil–water–gas multiphase flows by means of gamma-ray attenuation and artificial neural networks using one detector. *Measurement*, 51:34–41.

Roshani, G., Feghhi, S., and Setayeshi, S. (2015). Dual-modality and dual-energy gamma ray densitometry of petroleum products using an artificial neural network. *Radiation Measurements*, 82:154–162.

Roshani, G., Nazemi, E., and Roshani, M. (2017a). Flow regime independent volume fraction estimation in three-phase flows using dual-energy broad beam technique and artificial neural network. *Neural Computing and Applications*, 28(1):1265–1274.

Roshani, G., Nazemi, E., and Roshani, M. (2017b). Usage of two transmitted detectors with optimized orientation in order to three phase flow metering. *Measurement*, 100:122–130.

Salgado, C. M., Brandão, L. E., Schirru, R., et al. (2009). Prediction of volume fractions in three-phase flows using nuclear technique and artificial neural network. *Applied Radiation and Isotopes*, 67(10):1812–1818.

Salgado, C. M., Pereira, C. M., Schirru, R., et al. (2010). Flow regime identification and volume fraction prediction in multiphase flows by means of gamma-ray attenuation and artificial neural networks. *Progress in Nuclear Energy*, 52(6):555–562.

Takagi, T. and Sugeno, M. (1985). Fuzzy identification of systems and its applications to modeling and control. *IEEE Transactions on Systems, Man, and Cybernetics*, (1):116–132.

Thorn, R., Johansen, G., and Hammer, E. (1997). Recent developments in three-phase flow measurement. *Measurement Science and Technology*, 8(7):691.

Yousefi, T., Karami, A., Rezaei, E., et al. (2012). Fuzzy modeling of the forced convection heat transfer from a V-shaped plate exposed to an air slot jet. *Heat Transfer–Asian Research*, 41(5):430–443.